

## Drug Delivery

## Tissue-Penetrating, Hypoxia-Responsive Echogenic Polymersomes For Drug Delivery To Solid Tumors

Prajakta Kulkarni,<sup>[a]</sup> Manas K. Haldar,<sup>[a]</sup> Fataneh Karandish,<sup>[a]</sup> Matthew Confeld,<sup>[a]</sup> Rayat Hossain,<sup>[a]</sup> Pawel Borowicz,<sup>[b]</sup> Kara Gange,<sup>[c]</sup> Lang Xia,<sup>[d]</sup> Kausik Sarkar,<sup>[d]</sup> and Sanku Mallik\*<sup>[a]</sup>

**Abstract:** Hypoxia in solid tumors facilitates the progression of the disease, develops resistance to chemo and radiotherapy, and contributes to relapse. Due to the lack of tumor penetration, most of the reported drug carriers are unable to reach the hypoxic niches of the solid tumors. We have developed tissue-penetrating, hypoxia-responsive echogenic polymersomes to deliver anticancer drugs to solid tumors. The polymersomes are composed of a hypoxia-responsive azobenzene conjugated and a tissue penetrating peptide functionalized polylactic acid-polyethylene glycol polymer. The drug-encapsulated, hypoxia-responsive polymersomes substantially decreased the viability of pancreatic cancer cells in spheroidal cultures. Under normoxic conditions, polymersomes were echogenic at diagnostic ultrasound frequencies but lose the echogenicity under hypoxia. In-vivo imaging studies with xenograft mouse model further confirmed the ability of the polymersomes to target, penetrate, and deliver the encapsulated contents in hypoxic pancreatic tumor tissues.

Hypoxia or reduced oxygen partial pressure is observed in solid tumor tissues.<sup>[1]</sup> The high interstitial fluidic pressures and irregular blood flow lead to hypoxic regions in the tumors and help the progression of the disease.<sup>[2]</sup> Hypoxic niches further assist in the remodeling of the extracellular matrix<sup>[3]</sup> and changes in biochemical makeup, which drive tumor progression and the maintenance of the progenitor cancer stem

cells.<sup>[4]</sup> Solid tumors of breast, pancreas, cervix, rectum, head, and neck show hypoxic regions, making them difficult to treat.<sup>[5,6]</sup> However, the biochemical changes in the tumor microenvironment can be used as triggers for activating stimuli-responsive carriers and deliver drugs.<sup>[7]</sup> Biochemical triggers such as increased matrix metalloproteinase enzyme, glutathione, decreased pH are demonstrated to deliver the drugs from the carriers.<sup>[8]</sup> Hypoxia-responsive drug-delivery systems are comparatively less explored. Hypoxic niches are usually inaccessible to the circulating drugs due to lack of proximity to the vasculature.<sup>[9]</sup> Although the polyethylene glycol (PEG)-containing drug carriers extravasate through the leaky vasculature in the tumor tissues,<sup>[10]</sup> reaching the hypoxic regions requires subsequent tissue penetration.<sup>[11]</sup>

The cyclic iRGD peptide is known for its tissue-penetrating properties. It first binds to the integrin receptors on the cell surface. Subsequent hydrolysis and reduction generates a shorter peptide with high affinity for the neuropilin receptors and tissue penetration capability.<sup>[12]</sup> Nanoparticles conjugated to the iRGD peptide have been observed to penetrate into the tumors and deliver the drugs.<sup>[13,14]</sup> In an in vivo study, the chemotherapeutic drugs showed better efficacy when co-administered with the iRGD peptide.<sup>[15]</sup> We hypothesized that iRGD functionalized, PEGylated polymersomes will penetrate deep inside tumor tissues to reach the hypoxic regions. Subsequently, the hypoxia-responsive groups, incorporated in the polymersome bilayer would undergo reduction and destabilize the membrane integrity. Membrane destabilization will lead to the release of the encapsulated hydrophilic contents in the hypoxic tumor niches, causing cytotoxic effects. To test the hypothesis, we prepared azobenzene incorporated PLA-PEG polymer (Figure 1A) and mixed it with iRGD conjugated PLA-PEG polymer (Figure 1C) to form polymersomes by the solvent exchange method.<sup>[16]</sup> Azobenzene acts as a hypoxia-responsive linker and undergoes reduction in the hypoxic niches of the tumor microenvironment.<sup>[17]</sup> The ratio of hydrophilicity to hydrophobicity in an amphiphilic polymer is critical for the formation of polymersomes. Hence, we synthesized a PLA6000-azobenzene-PEG2000 copolymer with an appropriate balance between hydrophilic and hydrophobic polymer chains to form vesicle structures. We confirmed the azobenzene incorporation and the molecular weight of the synthesized polymer using NMR spectroscopy and gel permeation chromatography (GPC) (see the Supporting Information). To impart the tissue-penetrating property, hexynoic acid conjugated iRGD peptide (Fig-

[a] P. Kulkarni, Dr. M. K. Haldar, F. Karandish, M. Confeld, R. Hossain, Prof. S. Mallik  
Pharmaceutical Sciences, North Dakota State University  
Fargo, North Dakota 58105 (USA)  
E-mail: Sanku.Mallik@ndsu.edu

[b] Dr. P. Borowicz  
Department of Animal and Range Sciences  
North Dakota State University, Fargo, North Dakota 58105 (USA)

[c] Prof. K. Gange  
Department of Health, Exercise, and Nutrition Sciences  
North Dakota State University, Fargo, North Dakota 58105 (USA)

[d] L. Xia, Prof. K. Sarkar  
Mechanical and Aerospace Engineering  
George Washington University, Washington, DC 20052 (USA)

Supporting information and the ORCID identification number(s) for the author(s) of this article can be found under:  
<https://doi.org/10.1002/chem.201802229>

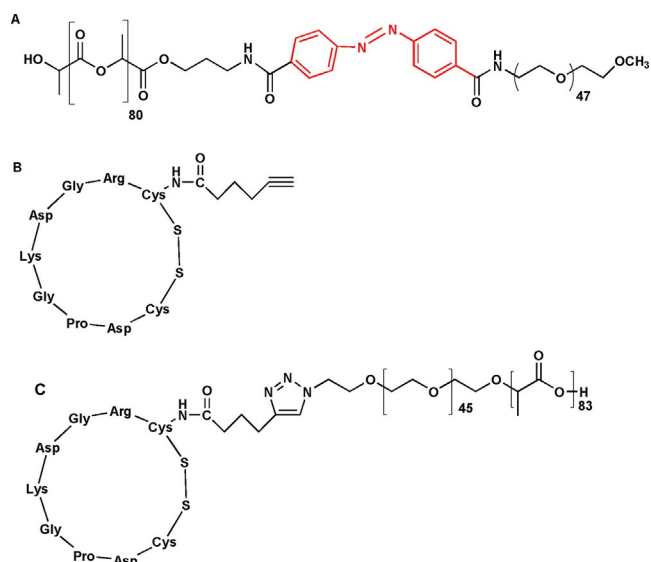


**Figure 1.** Structures for hypoxia responsive polymer (A), hexynoic acid conjugated iRGD peptide (B), and peptide iRGD conjugated PLA-PEG polymer (C). The hypoxia-sensitive azobenzene group is indicated in red.

ure 1B) was synthesized using a microwave-assisted peptide synthesizer (Liberty Blue, CEM Corporation) and conjugated to the synthesized PLA-PEG-N<sub>3</sub> polymer (Figure 1C). The MALDI mass spectrum (expected mass: 1042.43, Observed mass: 1042.36) and circular dichroism (CD) spectroscopy confirmed successful conjugation of the peptide to the amphiphilic copolymer.

We have used the iRGD peptide to enhance the tumor penetration of liposomes in the tumor tissues.<sup>[13]</sup> However, polymersomes are considerably more stable compared to the liposomes, and offer better membrane stability with reduced drug release in the absence of stimulus.<sup>[18]</sup> The polymer composition of the polymersomes was optimized by varying each component and determining the size and content release under hypoxic conditions. The optimized polymersome formulation was composed of PLA-azobenzene-PEG (90 mol%) and PLA-PEG-iRGD (10 mol%). We observed that the polymersomes prepared by the solvent exchange method were less than 200 nm in size. Exposure to hypoxia resulted in a reduction in size and increase in polydispersity index (PDI) value, indicating varied size distribution in the polymersomes (Figure S1, Table S1, Supporting Information). To further investigate the structural changes, we imaged the polymersomes by transmission electron microscopy (TEM). TEM imaging indicated the spherical shape of the polymersomes under normoxic conditions (Figure 2A). However, under hypoxia, the polymersome structures were disrupted (Figure 2B).

The ability of the polymersomes to release encapsulated contents under hypoxic conditions was studied by encapsulating the self-quenching dye carboxyfluorescein (100 mM) in the vesicles. The polymersomes released 85% of the encapsulated dye after 2-hour exposure to hypoxic conditions created in the presence of rat liver microsomes, NADPH (100 μM), and bubbling nitrogen gas. Under normoxia (no nitrogen gas bubbling), the release of the dye was less than 10%, indicating rel-

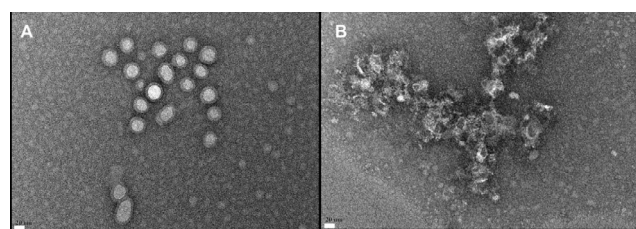


**Figure 2.** TEM images of polymersomes before (A) and after (B) exposure to hypoxia (scale bars indicate 20 nm).

ative stability of the polymersomes in the presence of oxygen (Figure S3).

Echogenic nanoparticles entrap air in their core or membranes and allow simultaneous ultrasound imaging.<sup>[19]</sup> We have demonstrated that incorporation of cryoprotectants during the preparation allows entrapment of air in the nanoparticles.<sup>[20]</sup> Echogenicity was induced in the iRGD functionalized polymersomes by using mannitol (320 mM) as the cryoprotectant. We carried out three freeze and thaw cycles to incorporate bubbles in the bilayer or the core (the exact location is unknown). We freeze-dried the polymersome solution and reconstituted with water for the ultrasound imaging employing a diagnostic frequency ultrasound scanner (Figure S4). The ultrasound reflection was observed in the echogenic polymersomes (mannitol-encapsulated) samples (0.1 mg mL<sup>-1</sup>), but not in the control samples (buffer-encapsulated polymersomes). Subsequently, the pancreatic cancer cells (BxPC-3) were cultured under normoxic and hypoxic environments. Monolayer cultures of BxPC-3 cells were incubated with the echogenic polymersomes under hypoxia for one hour and then imaged. We observed that, after one hour of hypoxia, the polymersomes showed decreased grayscale values in the ultrasound images indicating decreased echogenicity (Figure 3). The images analyzed by the NIH ImageJ software showed a three-fold decrease in the echogenicity after one hour of incubation in the hypoxic environment, suggesting disruption of polymer membrane and release of encapsulated air bubbles.

Because the iRGD peptide possesses anti-metastatic properties,<sup>[21]</sup> we evaluated the toxicity of the peptide-decorated vesicles towards pancreatic cancer cells. We observed 80% viability of the BxPC-3 cells in the presence of 100 μg mL<sup>-1</sup> concentration of the polymersomes (Figure 4). After confirming the echogenicity, stimuli-responsiveness, and the viability of the cells, we encapsulated the anticancer drug gemcitabine in the polymersomes (efficiency: 50%) using the pH-gradient method.<sup>[20]</sup> We treated monolayer cultures of BxPC-3 cells with the polymersomes encapsulating gemcitabine (20 μM) for 72 h. We used four controls to demonstrate the effectiveness of the gemcitabine-encapsulated, iRGD-conjugated, hypoxia-responsive vesicles: (C1) iRGD-conjugated, hypoxia-responsive test polymersomes encapsulating buffered saline only (i.e., no gemcitabine), (C2) gemcitabine-encapsulated, iRGD-conjugated polymersomes prepared from PLA6000-PEG2000 (devoid of hypoxia-responsive linker), (C3) gemcitabine-encapsulated, hypoxia-responsive polymersomes without the iRGD peptide, and (C4) un-encapsulated gemcitabine (20 μM) (Figure 4A).

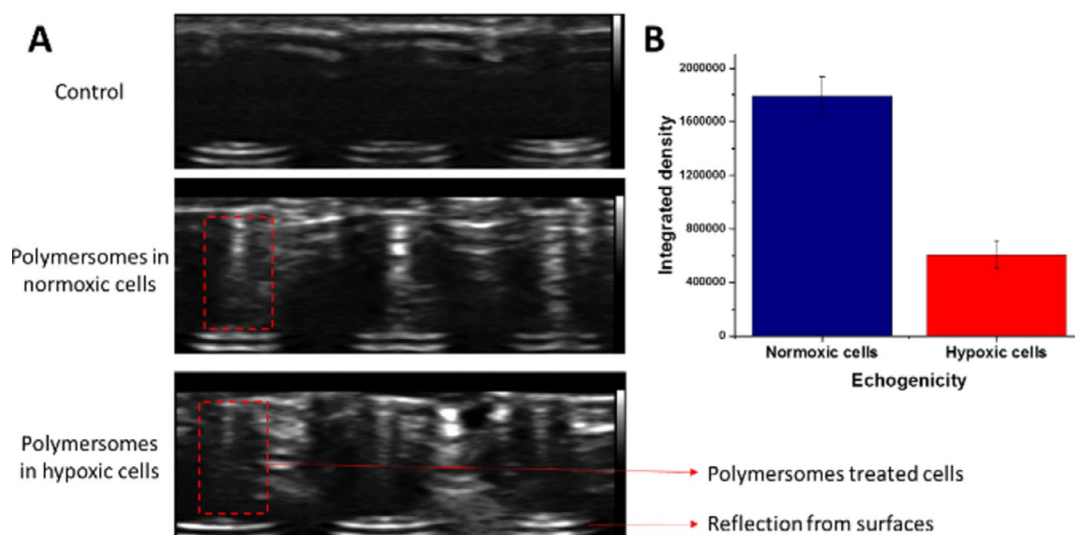


**Figure 3.** Ultrasound images of BxPC-3 cells treated with polymersomes under normoxic and hypoxic conditions in a 96-well plate (A). Change in grayscale value observed by the ImageJ software ( $n=3$ ) (B). The reduction in the grayscale value was after the hypoxic treatment indicated loss of echogenicity due to the disintegration of the polymersomes and release of contents (B).

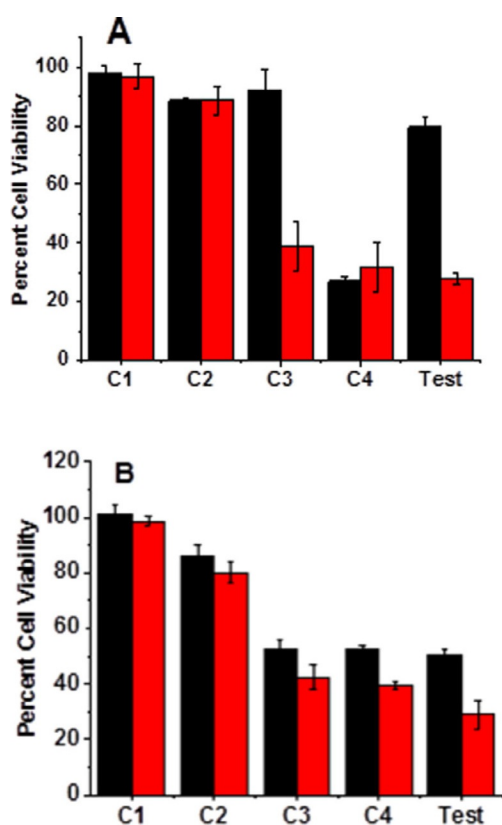


**Figure 4.** Cell viability in monolayer (A) and spheroidal (B) cultures of BxPC-3 cells after treatment with free gemcitabine, gemcitabine encapsulating control, and iRGD incorporated, gemcitabine encapsulated, hypoxia responsive polymersomes (Test) under normoxic (black bars) and hypoxic (red bars) environment. The controls are: (C1) iRGD-conjugated, hypoxia-responsive test polymersomes encapsulating buffered saline only (i.e., no gemcitabine), (C2) gemcitabine-encapsulated, iRGD-conjugated polymersomes prepared from PLA6000-PEG2000 (devoid of hypoxia-responsive linker), (C3) gemcitabine-encapsulated, hypoxia-responsive polymersomes without the iRGD peptide, and (C4) un-encapsulated gemcitabine ( $20\ \mu\text{M}$ ).

In hypoxic monolayer cultures of BxPC-3 cells, iRGD peptide conjugated hypoxia responsive polymersomes (Test, red column, Figure 4A) showed a decreased cell viability of 25%, similar to the cytotoxicity of free gemcitabine (C4, red column). The results indicate that nearly all of the encapsulated gemcitabine is released from the polymersomes under hypoxia. In addition, these polymersomes showed less effectiveness under normoxic conditions (Test, black column, cell viability: 80%), demonstrating the role of hypoxia in releasing the encapsulated gemcitabine from the vesicles. The vesicles devoid of the hypoxia-responsive polymer (i.e., prepared from PLA6000-PEG2000; C2) showed high cell viability (82%), which further confirmed the stimuli-responsive release of the gemcitabine from the vesicles (Figure 4A).

The reduced vasculature in the pancreatic tumors rapidly gives rise to the hypoxic niches. The development of hypoxia is commonly associated with disease progression, poor prognosis, and impaired therapeutic response.<sup>[23]</sup> In-vitro studies with monolayer cultures do not provide realistic predictions about the efficacy of the drug carrier.<sup>[24]</sup> The three-dimensional (3D) spheroid cultures are better in vitro models for testing drug delivery systems.<sup>[25]</sup> We cultured 3D spheroids of BxPC-3 cells and treated them with the polymersome formulations. The spheroidal cultures under normoxia showed decreased cell viability in the presence of hypoxia-responsive polymersomes encapsulating gemcitabine (52%; Figure 4B, Test, black column). Cell spheroids often exhibit hypoxia in the core.<sup>[25]</sup> We speculate that decrease in the cell viability under normoxic conditions may be due to iRGD peptide-assisted penetration of the vesicles to the hypoxic niches and subsequent release of gemcitabine. However, the targeted, drug-encapsulated polymersomes were more effective in the spheroids of the pancreatic cancer cells compared to the monolayer cultures (Figure 4B, Test, red column). In fact, the gemcitabine released from the targeted, hypoxia-responsive polymersomes (Test

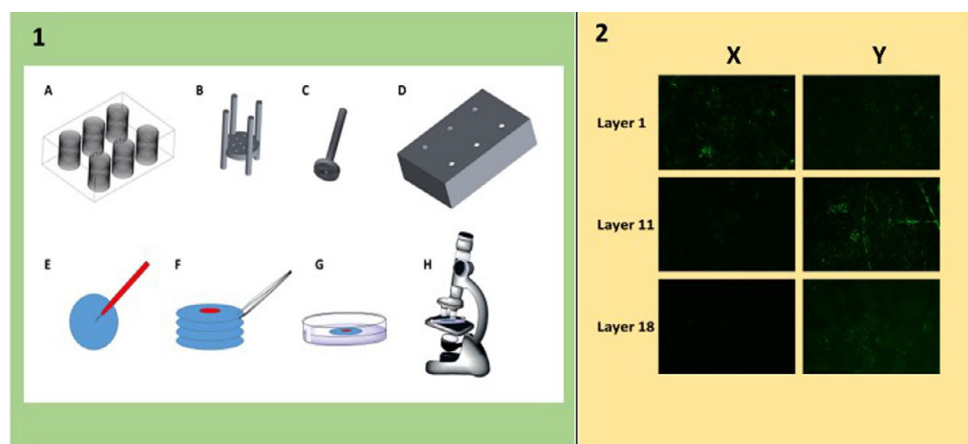


**Figure 5.** Designed, 3D-printed cell culture apparatus (1A) in which a paper stack holder (1B) was paced with a press on the top of the stack with a hollow tubing (1C) enclosed by the cover (1D). Whatman filter was inoculated with BxPC-3 cells embedded in sodium alginate and agarose (1E), and the filter papers were stacked together (1F), and the stack was allowed to grow in the apparatus. For imaging, each stacked paper was separated (1F) and placed in a clear glass bottom Petri plate (1G) to image under a laser-scanning confocal microscope (1H). The depth of penetration of hypoxia-responsive polymersomes before (2X) and after iRGD conjugation (2Y). The green color in Panel 2 indicates the carboxyfluorescein dye, released from the polymersomes.

column, red bar) were more effective compared to the free drug (column C4, red bar), possibly due to the higher penetration depth of the targeted vesicles.

To determine the iRGD assisted penetration depth of the polymersomes, cell layers were cultured on the wet strengthened Whatman filter papers (#114) employing an in-house, 3D-printed culture apparatus (Figure 5).<sup>[26]</sup> When layered cultures were treated with the carboxyfluorescein encapsulated polymersomes, we observed that vesicles without iRGD-peptide penetrated 11 layers of the stacked cells. However, the iRGD peptide-decorated polymersomes penetrated up to 18th layer (2.2 mm), indicating the ability to penetrate deep inside cellular systems (Figure 5).

To demonstrate active targeting of the peptide-decorated polymersomes and hypoxia-triggered release *in vivo*, we developed xenografts of pancreatic cancer in male nude mice by subcutaneously injecting the BxPC-3 cells ( $10^6$ ). After four weeks of tumor development, we injected the hypoxia-sensitive dye Image-iT (Thermo Fisher Scientific) encapsulated, hypoxia-responsive, iRGD-decorated polymersomes in three mice through the tail vein.<sup>[28]</sup> After two hours, we imaged the animals employing a Kodak reflectance imager (excitation: 490 nm; detector: 620 nm). As the fluorescence of the dye is activated only under hypoxia, fluorescence at the tumor site was indicative of the release of the dye from the polymersomes and subsequent activation under hypoxic conditions. We observed that the polymersomes accumulate in the tumor and release the dye (Figure 6B). We did not observe any release of the dye when the iRGD peptide-decorated polymersomes lacked the hypoxia-responsive polymer (vesicles prepared from the polymer PEG2000-PLA6000, Figure 6A).

In pancreatic cancer, hypoxia promotes the development of collagen-rich, fibrous extracellular stroma, which limits the diffusion and transport of the drugs to the tumor mass.<sup>[27]</sup> To determine the penetration depth of iRGD polymersomes in pancreatic tumors, we used mice growing pancreatic tumors xenograft of BxPC-3 cells as described in the previous paragraph.

After four weeks of tumor development, we injected the non-hypoxia responsive polymersomes (prepared from PLA6000-PEG2000) presenting the iRGD peptide through the tail vein of three mice. The vesicles incorporated a fluorescent lipid in the bilayer for imaging (DPPE-lissamine rhodamine B, excitation: 560 nm; emission: 585 nm). After two hours, the mice were euthanized, the tumors were excised, snap-frozen, and sliced. We imaged a slice of the tumor, 200  $\mu\text{m}$  from the surface (Figure 6C) using a fluorescence microscope. The red fluorescence (indicated by arrows) demonstrated that the iRGD-polymersomes penetrated at least 200  $\mu\text{m}$  into the pancreatic tumor in mice.<sup>[29]</sup>

To demonstrate the proof of concept, we injected the echogenic polymersomes (100  $\mu\text{L}$ ) in an anesthetized live female nude mouse via the tail vein. A highly perfused organ (right kidney) was then imaged with a live animal ultrasound imaging instrument (VisualSonics, Vevo3100) at 40 MHz transducer frequency. The preliminary data indicated contrast enhance-

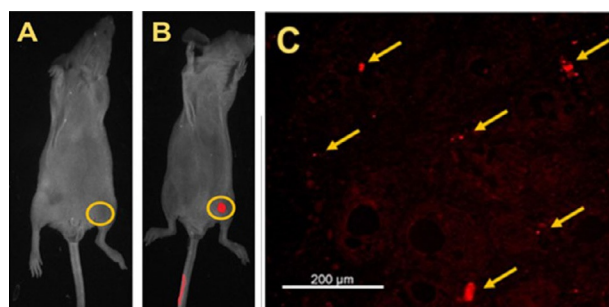


**Figure 6.** Imaging of hypoxic pancreatic tumor in mice and penetration depth of the iRGD polymersomes. The release of the hypoxia-responsive dye Image-iT from hypoxia-sensitive polymersomes was observed after two hours (B) of injection via the tail vein in nude mice. No dye release was observed when the polymersomes lacked the hypoxia-responsive linker (A). The yellow circles represent the tumor in the mice. (C) Fluorescence microscopic image of a 5  $\mu\text{m}$  thick slice, 200  $\mu\text{m}$  from the top surface of the excised tumor, showing the presence of the iRGD-decorated vesicles (indicated by arrows).

ment compared to the control (without any injected polymerosomes, Figure S7 in the Supporting Information). We are currently optimizing the conditions to increase the contrast of the ultrasound image of the live animal.

In conclusion, iRGD peptide functionalized hypoxia responsive polymerosomes encapsulated the anticancer drug gemcitabine with 50% efficiency. The polymerosomes successfully released the encapsulated contents in vitro and in vivo. Treatment with these polymerosomes significantly improved the depth of penetration while decreasing cell viability under hypoxic conditions. These polymerosomes were observed to be echogenic in ultrasound imaging. In vivo imaging experiments confirmed the improved targeting and release of the contents in the hypoxic tissues of mice growing xenograft tumors of pancreatic cancer cells. We have demonstrated that echogenic, iRGD-decorated hypoxia-responsive polymerosomes can be used for imaging of hypoxia and deliver the drugs to the hypoxic regions of the pancreatic tumor tissues.

## Acknowledgements

The animal experiments were conducted following the protocol approved by the Institutional Animal Care and Use Committee of North Dakota State University (Protocol Number: A16057). This research was supported by NIH grant 1 R01GM114080 to SM and KS. SM also acknowledges support from the Grand Challenge Initiative and the Office of the Vice President for Research and Creative Activity, North Dakota State University. We acknowledge the Animal Studies Core Facility supported through the COBRE Center for Diagnostic and Therapeutic Strategies in Pancreatic Cancer (1 P20GM109024).

## Conflict of interest

The authors declare no conflict of interest.

**Keywords:** drug delivery · hypoxia · pancreatic cancer · polymers · polymerosomes

- [1] P. Vaupel, L. Harrison, *Oncologist* **2004**, *9*, 4–9.  
 [2] C.-H. Heldin, K. Rubin, K. Pietras, A. Östman, *Nat. Rev. Cancer* **2004**, *4*, 806–813.  
 [3] D. M. Gilkes, G. L. Semenza, D. Wirtz, *Nat. Rev. Cancer* **2014**, *14*, 430–439.  
 [4] S. M. Pupa, S. Ménard, S. Forti, E. Tagliabue, *J. Cell. Physiol.* **2002**, *192*, 259–267.

- [5] B. A. Teicher, *Cancer Metastasis Rev.* **1994**, *13*, 139–168.  
 [6] P. Vaupel, D. K. Kelleher, M. Höckel, in *Seminars in Oncology*, Vol. 28, Elsevier, **2001**, pp. 29–35.  
 [7] S. Ganta, H. Devalapally, A. Shahiwala, M. Amiji, *J. Controlled Release* **2008**, *126*, 187–204.  
 [8] S. R. MacEwan, D. J. Callahan, A. Chilkoti, *Nanomedicine* **2010**, *5*, 793–806.  
 [9] S. Kizaka-Kondoh, M. Inoue, H. Harada, M. Hiraoka, *Cancer Sci.* **2003**, *94*, 1021–1028.  
 [10] H. Maeda, G. Bharate, J. Daruwalla, *Eur. J. Pharmac. Biopharmac.* **2009**, *71*, 409–419.  
 [11] W. R. Wilson, M. P. Hay, *Nat. Rev. Cancer* **2011**, *11*, 393–410.  
 [12] T. Teesalu, K. N. Sugahara, E. Ruoslahti, *Front. Oncol.* **2013**, *3*, 216.  
 [13] P. Kulkarni, M. K. Haldar, P. Katti, C. Dawes, S. You, Y. Choi, S. Mallik, *Bioconjugate Chem.* **2016**, *27*, 1830–1838.  
 [14] G. Gu, X. Gao, Q. Hu, T. Kang, Z. Liu, M. Jiang, D. Miao, Q. Song, L. Yao, Y. Tu, *Biomaterials* **2013**, *34*, 5138–5148.  
 [15] K. N. Sugahara, T. Teesalu, P. P. Karmali, V. R. Kotamraju, L. Agemy, D. R. Greenwald, E. Ruoslahti, *science* **2010**, *328*, 1031–1035.  
 [16] R. Nahire, M. K. Haldar, S. Paul, A. H. Ambre, V. Meghnani, B. Layek, K. S. Katti, K. N. Gange, J. Singh, K. Sarkar, S. Mallik, *Biomaterials* **2014**, *35*, 6482–6497.  
 [17] A. Chevalier, W. Piao, K. Hanaoka, T. Nagano, P.-Y. Renard, A. Romieu, *Methods and Applicat. Fluores.* **2015**, *3*, 044004.  
 [18] H. Y. Chang, Y. J. Sheng, H. K. Tsao, *Soft Matter* **2014**, *10*, 6373–6381.  
 [19] O. Diou, N. Tsapis, E. Fattal, *Expert Opin. Drug Delivery* **2012**, *9*, 1475–1487.  
 [20] S. Paul, R. Nahire, S. Mallik, K. Sarkar, *Comput. Mech.* **2014**, *53*, 413–415.  
 [21] K. N. Sugahara, G. B. Braun, T. H. de Mendoza, V. R. Kotamraju, R. P. French, A. M. Lowy, T. Teesalu, E. Ruoslahti, *Molecular Cancer Therapeutics* **2015**, *14*, 120–128.  
 [22] M. Grazia Calvagno, C. Celia, D. Paolino, D. Cosco, M. Iannone, F. Castelli, P. Doldo, M. Frest, *Current Drug Delivery* **2007**, *4*, 89–101.  
 [23] a) P. Dauer, A. Nomura, A. Saluja, S. Banerjee, *Pancreatology* **2017**, *17*, 7–12; b) M. Erkan, M. Kurtoglu, J. Kleeff, *Expert Review of Gastroenterology & Hepatology* **2016**, *10*, 301–316; *Hepatology* **2016**, *10*, 301–316.  
 [24] A. Khoruzhenko, *Biopolymers and Cell*, **2011**, *27*, 17–24.  
 [25] Y.-C. Tung, A. Y. Hsiao, S. G. Allen, Y.-s. Torisawa, M. Ho, S. Takayama, *Analyst* **2011**, *136*, 473–478.  
 [26] R. Derda, A. Laromaine, A. Mammoto, S. K. Tang, T. Mammoto, D. E. Ingber, G. M. Whitesides, *Proc. Natl. Acad. Sci. USA* **2009**, *106*, 18457–18462.  
 [27] a) S. Lunardi, R. J. Muschel, T. B. Brunner, *Cancer Lett.* **2014**, *343*, 147–155; b) V. Heinemann, M. Reni, M. Ychou, D. J. Richel, T. Macarulla, M. Ducreux, *Cancer Treat. Rev.* **2014**, *40*, 118–128.  
 [28] S. Zhang, M. Hosaka, T. Yoshihara, K. Negishi, Y. Iida, S. Tobita, T. Takeuchi, *Cancer Res.* **2010**, *70*, 4490–4498.  
 [29] X. Xu, J. Wu, Y. Liu, M. Yu, L. Zhao, X. Zhu, S. Bhasin, Q. Li, E. Ha, J. Shi, O. C. Farokhzad, *Angew. Chem. Int. Ed.* **2016**, *55*, 7091–7094; *Angew. Chem.* **2016**, *128*, 7207–7210.

Manuscript received: May 3, 2018  
 Revised manuscript received: June 22, 2018  
 Accepted manuscript online: July 2, 2018  
 Version of record online: July 30, 2018